

CLIP-RD : Relative Distillation for Efficient CLIP Knowledge Distillation

Jeannie Chung*, Hanna Jang*, Ingyeong Yang*, Uiwon Hwang[†], Jaehyeong Sim[†]
Ewha Womans University, Seoul 03760, South Korea
uiwon.hwang@ewha.ac.kr, jh.sim@ewha.ac.kr

* Equal contribution [†] Corresponding authors

Abstract

CLIP aligns image and text embeddings via contrastive learning and demonstrates strong zero-shot generalization. Its large-scale architecture requires substantial computational and memory resources, motivating the distillation of its capabilities into lightweight student models. However, existing CLIP distillation methods do not explicitly model multi-directional relational dependencies between teacher and student embeddings, limiting the student’s ability to preserve the structural relationships encoded by the teacher. To address this, we propose a relational knowledge distillation framework that introduces two novel methods, Vertical Relational Distillation (VRD) and Cross Relational Distillation (XRD). VRD enforces consistency of teacher–student distillation strength across modalities at the distribution level, while XRD imposes bidirectional symmetry on cross-modal teacher–student similarity distributions. By jointly modeling multi-directional relational structures, CLIP-RD promotes faithful alignment of the student embedding geometry with that of the teacher, outperforming existing methods by 0.8%*p*.

1 Introduction

CLIP is one of the most representative vision-language models, jointly encoding both image and text inputs into a shared embedding space [34]. Trained on 400 million image-text pairs via contrastive learning, it achieves strong generalization capability across diverse downstream tasks. It has dramatically changed the paradigm of vision-language models, with its adoption expanding beyond simple image classification into tasks such as object detection [1, 40] and visual question answering [4, 8]. This widespread adoption, however, comes with a significant computational cost, as its large-scale architecture demands substantial memory and processing resources. This has naturally driven the demand for lightweight alternatives that can preserve these capabilities at a reduced cost.

To this end, knowledge distillation (KD) [19] has gained considerable attention as an effective model compression technique [7, 28, 6, 55]. It transfers knowledge from a large teacher model to a smaller student model, allowing the student model to inherit the capabilities of the teacher model. In other words, via a single distillation process, a compact student model can transfer comparable performance from the teacher despite its significantly fewer parameters. The definition of knowledge varies depending on the task and model architecture. For instance, in classification tasks [19], knowledge is commonly represented as soft logits produced after the softmax layer, carefully designed to best reflect the characteristics of the target task.

Knowledge distillation for CLIP is a challenging task, as it requires transferring both features and their relationships from teacher to student. Many prior works have attempted to distill CLIP in various ways. TinyCLIP [49] leverages affinity mimicking and compresses a teacher CLIP model into a student via weight inheritance, achieving strong performance. However, it requires the teacher and student to share the same architecture, which limits its practical applicability. To address this, CLIP-KD [52] proposes a new framework that distills features and contrastive relations between image-text pairs, achieving state-of-the-art zero-shot accuracy on ImageNet.

Specifically, CLIP-KD [52] introduces three core distillation components: Feature Distillation (FD), Interactive Contrastive Learning (ICL), and Contrastive Relational Distillation (CRD). Among them, CRD aligns image-to-text similarity distributions within the model, approximating the student’s distributions toward those of the teacher, enabling the student to learn the relational structure of the teacher’s embeddings. As illustrated in Figure 1-(a), we refer to CRD as Horizontal Relational Distillation (HRD) throughout this paper since it aligns horizontal relational structures. However, it relies solely on unidirectional relational distillation, which limits effective alignment in the student’s representation space. To overcome this limitation, we propose CLIP-RD.

We consider relational structures between the teacher

and student as well as across modalities as the primary knowledge to be distilled from the multimodal teacher. To capture and transfer these structures, we introduce Vertical Relational Distillation (VRD) and Cross Relational Distillation (XRD). This formulation explicitly models the multi-directional dependencies between the teacher and the student. VRD aligns vertically-directed similarity distributions using two losses, as shown in Figure 1-(b): contrastive loss and KL-divergence loss. We maximize the similarity between teacher and student embeddings via contrastive loss, and further align these distributions with KL-divergence loss, enforcing consistency in teacher-student distillation strength across modalities at the distribution level. XRD aligns cross-directed similarity distributions, as shown in Figure 1-(c), by constructing teacher text–student image and teacher image–student text pairs, and minimizing their KL-divergence. Through XRD, we enforce bidirectional symmetry in cross-modal teacher-student similarity distributions.

With these two novel strategies together with HRD, we are able to model multi-directional relational distributions: horizontal, vertical, and cross, as illustrated in Figure 1-(d). Through this multi-directional framework, we effectively align the student’s representation space and transfer CLIP’s strong generalization capabilities to the student model. In our experiments, we use a CLIP model with a ViT-B/16 [10] pre-trained on LAION-400M [38], then distill its knowledge into a lightweight ViT-T/16 student model using CC3M [39] and CC12M [3] datasets. We evaluate the student model on ImageNet [9] for zero-shot classification and on MSCOCO [29] and Flickr30K [53] for zero-shot retrieval. Our proposed method, CLIP-RD, outperforms CLIP-KD by 0.8%p on ImageNet zero-shot classification, demonstrating the effectiveness of our multi-directional relational distillation framework.

Our main contributions are as follows:

- We identify that existing CLIP distillation methods rely on unidirectional relational distillation, which limits effective alignment in the student representation space. To address this limitation, we propose CLIP-RD, a unified multi-directional relational distillation framework.
- We propose Vertical Relational Distillation (VRD) and Cross Relational Distillation (XRD), which jointly model bidirectional symmetry across modalities and cross-modal teacher–student alignment by enforcing distribution-level consistency.
- Our method achieves 42.1% zero-shot classification on ImageNet, outperforming CLIP-KD by 0.8%p, and demonstrates competitive performance on zero-shot retrieval benchmarks including MSCOCO and Flickr30K.

2 Related Work

2.1 Knowledge Distillation

The recent evolution of large-scale models has achieved unprecedented performance across various tasks, largely driven by scaling laws [22], where model capabilities improve with increased parameter count, dataset size, and computational resources. Despite these advances, their significant latency and resource demands [44] have made improving model efficiency an active area of research [24, 25, 36, 21, 42, 50] across diverse tasks [7, 13, 46] and modalities [42, 50, 31, 36, 21]. Knowledge Distillation (KD) [19] has emerged as a key paradigm. KD transfers rich representations from a high-capacity teacher to a compact student, allowing the student to achieve superior performance despite the limitations of its smaller architecture. Although KD was initially established within the context of unimodal models [21, 50], researchers have recently extended these methodologies to Vision-Language Models (VLMs) [7, 28, 6, 55]. In this work, we address the limited exploration of relational structures in multi-modal distillation by focusing on knowledge transfer that preserves cross-modal relationships.

2.2 CLIP

CLIP [34], introduced by OpenAI, is a Vision-Language Model (VLM) trained through contrastive learning to learn rich representations. The core objective of CLIP is to optimize a symmetric contrastive alignment loss, which pulls the embeddings of paired image-text samples closer while pushing unpaired samples apart in a shared embedding space. This alignment enables CLIP to achieve strong zero-shot generalization [47, 15, 34, 33, 54] across various downstream tasks [27, 32, 48], such as image classification [56, 20, 12] and cross-modal retrieval [11, 12], often outperforming existing VLMs [34].

As demand for efficient VLMs increases, KD has been widely used to compress large-scale pre-trained CLIP models [52, 49, 28, 6, 55]. In this context, most existing methods focus primarily on distilling feature-level representations rather than preserving relational structures between image-text pairs and teacher-student embeddings. Motivated by this, we propose two distillation strategies to preserve intra- and inter-modal relationships.

2.3 CLIP-KD

A notable advancement in compressing Vision-Language Models is CLIP-KD [52], which introduces a comprehensive framework incorporating feature, relation, gradient, and contrastive paradigms. Rather than relying on a single objective, CLIP-KD empirically determines effective combinations of various distillation strategies. However, it still fails to fully capture relational distillation. Building

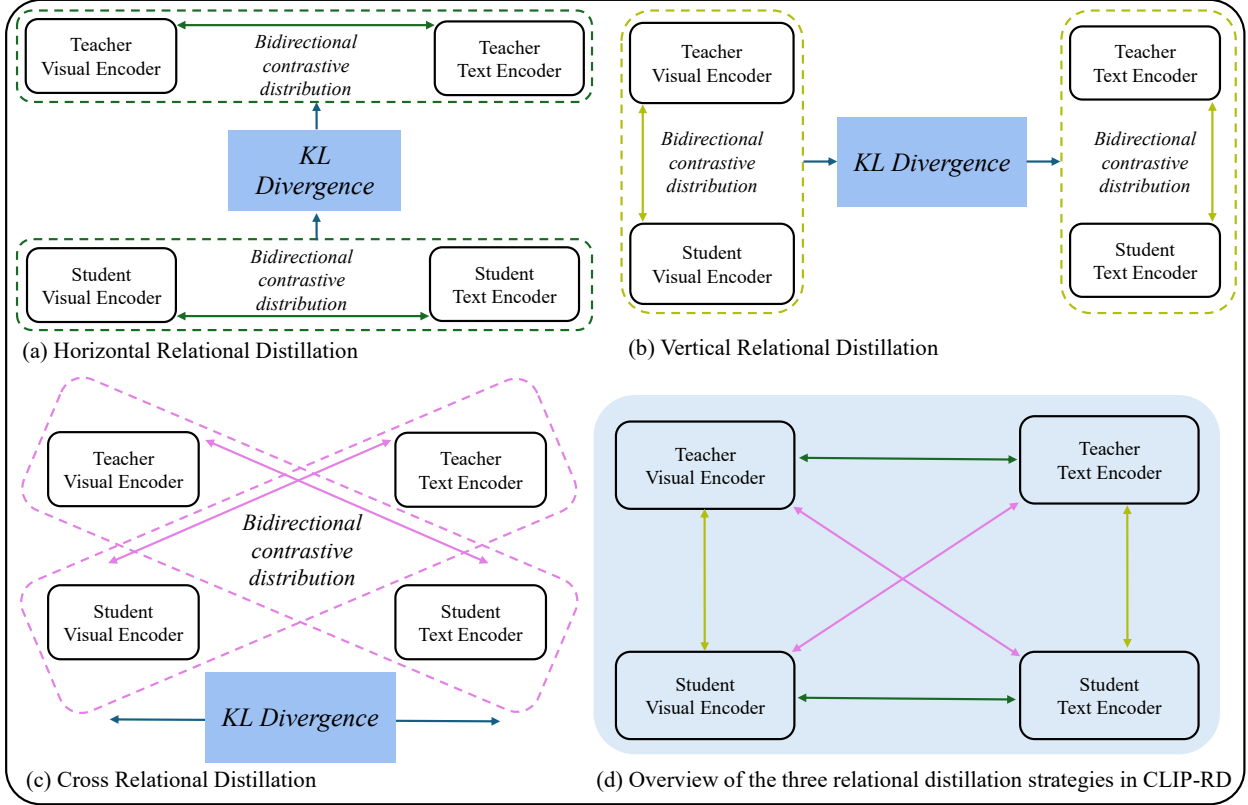


Figure 1: Overview of CLIP-RD.

upon the robust framework, we advance the state-of-the-art by intensifying the precision of relational alignment. Our methodology extends these foundations to more precisely distill the intricate relations between embeddings.

2.4 TinyCLIP

TinyCLIP [49] is one of the early works on multimodal knowledge distillation for compressing the CLIP framework. It encourages the student model to mimic the teacher’s cross-modal alignment in the image-text similarity space, primarily through distribution-level matching. TinyCLIP also employs weight inheritance and a multi-stage distillation strategy. However, its framework largely relies on architectural compatibility between the teacher and student models [52]. In contrast, our method explicitly focuses on relational alignment, leading to consistently stronger zero-shot performance across multiple benchmarks.

3 Methodology

In this section, we present the CLIP-RD framework, comprising two novel distillation strategies, VRD and XRD. We denote v_k^T and v_k^S as the image embedding vectors

from the teacher and student, respectively, and s_k^T and s_k^S as the corresponding text embeddings. Given a mini-batch $\mathcal{B} = \{(I_k, T_k)\}_{k=1}^{|\mathcal{B}|}$ where I_k and T_k denote the image and text of the k -th pair, respectively, we compute the relational distributions over these embedding vectors.

3.1 Overview of CLIP

CLIP establishes a joint embedding space for images and texts through contrastive learning on large-scale paired data. Specifically, CLIP employs an InfoNCE-based loss as its main training objective, aligning the representation of image-text pairs by maximizing the similarity of positive pairs while minimizing that of negative pairs. Formally, the CLIP loss, $\mathcal{L}_{\text{CLIP}}$, consists of two contrastive losses, $\mathcal{L}_{I \rightarrow T}$ and $\mathcal{L}_{T \rightarrow I}$, which measure the similarity using image and text as anchors, respectively:

$$\mathcal{L}_{I \rightarrow T} = -\log \frac{\exp(v_k \cdot s_k / \tau)}{\sum_{b=1}^{|\mathcal{B}|} \exp(v_k \cdot s_b / \tau)} \quad (1)$$

$$\mathcal{L}_{T \rightarrow I} = -\log \frac{\exp(s_k \cdot v_k / \tau)}{\sum_{b=1}^{|\mathcal{B}|} \exp(s_k \cdot v_b / \tau)} \quad (2)$$

Consequently, the total CLIP loss is defined as the average of the two. In our framework, we adopt this $\mathcal{L}_{\text{CLIP}}$ as

the task loss to preserve the fundamental alignment objective of the original CLIP model, and build our relational distillation strategies on top of it.

$$\mathcal{L}_{\text{task}} = \mathcal{L}_{\text{CLIP}} = \frac{1}{2} (\mathcal{L}_{I \rightarrow T} + \mathcal{L}_{T \rightarrow I}). \quad (3)$$

3.2 Background of CLIP-KD

Various knowledge distillation (KD) losses are often used to obtain smaller and more efficient student models via distillation from a large CLIP teacher. Losses proposed in CLIP-KD [52] transfer different aspects of the teacher’s knowledge.

Feature Distillation (FD): Simply aligns feature embeddings between teacher and student within the same modality.

$$\mathcal{L}_{\text{FD}} = \frac{1}{|\mathcal{B}|} \sum_{k=1}^{|\mathcal{B}|} \left(\|v_k^T - v_k^S\|_2^2 + \|s_k^T - s_k^S\|_2^2 \right). \quad (4)$$

Interactive Contrastive Learning (ICL): By contrasting student embeddings from one modality with teacher embeddings from another modality, we let the student learn the relationships between modalities.

$$\mathcal{L}_{\text{ICL}, I \rightarrow T} = -\log \frac{\exp(v_k^S \cdot s_k^T / \tau)}{\sum_{b=1}^{|\mathcal{B}|} \exp(v_k^S \cdot s_b^T / \tau)}. \quad (5)$$

Similarly, the text-to-image objective is:

$$\mathcal{L}_{\text{ICL}, T \rightarrow I} = -\log \frac{\exp(s_k^S \cdot v_k^T / \tau)}{\sum_{b=1}^{|\mathcal{B}|} \exp(s_b^S \cdot v_k^T / \tau)}. \quad (6)$$

The total ICL loss is defined as the average of $\mathcal{L}_{\text{ICL}, I \rightarrow T}$ and $\mathcal{L}_{\text{ICL}, T \rightarrow I}$:

$$\mathcal{L}_{\text{ICL}} = \frac{1}{2} (\mathcal{L}_{\text{ICL}, I \rightarrow T} + \mathcal{L}_{\text{ICL}, T \rightarrow I}) \quad (7)$$

Horizontal Relational Distillation (HRD): As shown in Figure 1, HRD transfers the horizontal relational structure to student, by aligning the horizontally-directed similarity distributions. HRD enables the student to learn well-structured semantic relationships, thereby improving the quality of its feature representations.

$$p_k^T[j] = \frac{\exp(v_k^T \cdot s_j^T / \tau^T)}{\sum_{b=1}^{|\mathcal{B}|} \exp(v_k^T \cdot s_b^T / \tau^T)}, \quad (8)$$

$$p_k^S[j] = \frac{\exp(v_k^S \cdot s_j^S / \tau^S)}{\sum_{b=1}^{|\mathcal{B}|} \exp(v_k^S \cdot s_b^S / \tau^S)}. \quad (9)$$

$$q_k^T[j] = \frac{\exp(s_k^T \cdot v_j^T / \tau^T)}{\sum_{b=1}^{|\mathcal{B}|} \exp(s_k^T \cdot v_b^T / \tau^T)} \quad (10)$$

$$q_k^S[j] = \frac{\exp(s_k^S \cdot v_j^S / \tau^S)}{\sum_{b=1}^{|\mathcal{B}|} \exp(s_k^S \cdot v_b^S / \tau^S)} \quad (11)$$

p_k^M for $M \in \{S, T\}$ is a probability distribution calculated based on the similarity with all $\{s_j\}_{j=1}^{|\mathcal{B}|}$ in the batch, with v_k as the anchor. Similarly, q_k^M is a probability distribution calculated based on the similarity with all $\{v_j\}_{j=1}^{|\mathcal{B}|}$ in the batch, with s_k as the anchor.

$$\mathcal{L}_{\text{HRD}, I \rightarrow T} = \frac{1}{|\mathcal{B}|} \sum_{k=1}^{|\mathcal{B}|} \sum_{j=1}^{|\mathcal{B}|} p_k^T[j] \log \frac{p_k^T[j]}{p_k^S[j]} \quad (12)$$

$$\mathcal{L}_{\text{HRD}, T \rightarrow I} = \frac{1}{|\mathcal{B}|} \sum_{k=1}^{|\mathcal{B}|} \sum_{j=1}^{|\mathcal{B}|} q_k^T[j] \log \frac{q_k^T[j]}{q_k^S[j]} \quad (13)$$

$$\mathcal{L}_{\text{HRD}} = \mathcal{L}_{\text{HRD}, I \rightarrow T} + \mathcal{L}_{\text{HRD}, T \rightarrow I} \quad (14)$$

Through KL divergence, the student effectively imitates the teacher’s horizontal relational structure across text and visual embeddings. This allows the student to mimic better structured semantic relations from the teacher, thereby improving the quality of feature representations.

By combining this HRD with VRD and XRD, introduced in the following sections, CLIP-RD achieves explicit modeling of multi-directional relational dependencies.

3.3 Vertical Relational Distillation (VRD)

We introduce Vertical Relational Distillation (VRD), a distillation strategy that enforces consistency of teacher–student distillation strength across modalities at the distribution level. As illustrated in Figure 1, VRD exploits two vertically-directed similarity distributions: image–image and text–text contrastive distributions. Specifically, we construct these distributions using both teacher and student as anchors. Given the image and text embeddings and learnable temperature parameters for each modality, each contrastive distribution is formulated as:

$$I_k^{TS}[j] = \frac{\exp(v_k^T \cdot v_j^S / \tau^i)}{\sum_{b=1}^{|\mathcal{B}|} \exp(v_k^T \cdot v_b^S / \tau^i)} \quad (15)$$

$$I_k^{ST}[j] = \frac{\exp(v_k^S \cdot v_j^T / \tau^i)}{\sum_{b=1}^{|\mathcal{B}|} \exp(v_k^S \cdot v_b^T / \tau^i)} \quad (16)$$

$$T_k^{TS}[j] = \frac{\exp\left(s_k^T \cdot s_j^S / \tau^t\right)}{\sum_{b=1}^{|\mathcal{B}|} \exp\left(s_k^T \cdot s_b^S / \tau^t\right)} \quad (17)$$

$$T_k^{ST}[j] = \frac{\exp\left(s_k^S \cdot s_j^T / \tau^t\right)}{\sum_{b=1}^{|\mathcal{B}|} \exp\left(s_k^S \cdot s_b^T / \tau^t\right)} \quad (18)$$

To effectively transfer these relational structures, VRD comprises two complementary losses: a contrastive loss and a KL-divergence loss. For the contrastive loss, we adopt an InfoNCE-based objective applied to each intra-modality distribution, maximizing the similarity between teacher and student embeddings of the same modality. Specifically, we compute this loss separately for each modality as $\mathcal{L}_{\text{CE-Image}}$ and $\mathcal{L}_{\text{CE-Text}}$. For $\mathcal{L}_{\text{CE-Image}}$, we leverage two image-image similarity distributions, using the teacher and student as anchors respectively, and sum the resulting losses. $\mathcal{L}_{\text{CE-Text}}$ follows the same formulation using text-text distributions. Finally, $\mathcal{L}_{\text{VRD-CE}}$ is obtained by averaging $\mathcal{L}_{\text{CE-Image}}$ and $\mathcal{L}_{\text{CE-Text}}$. Given the intra-modality distributions, $\mathcal{L}_{\text{VRD-CE}}$ is formulated as:

$$\mathcal{L}_{\text{CE-Image}} = -\log I_k^{TS}[k] - \log I_k^{ST}[k] \quad (19)$$

$$\mathcal{L}_{\text{CE-Text}} = -\log T_k^{TS}[k] - \log T_k^{ST}[k] \quad (20)$$

$$\mathcal{L}_{\text{VRD-CE}} = \frac{1}{2} (\mathcal{L}_{\text{CE-Image}} + \mathcal{L}_{\text{CE-Text}}) \quad (21)$$

Subsequently, we apply KL-divergence loss to align the intra-modality similarity distributions. This loss approximates the image similarity distribution to the text similarity distribution. This encourages consistent distillation strength between the teacher and student across modalities. Specifically, we apply this loss to both teacher-anchored and student-anchored distributions and average them to obtain $\mathcal{L}_{\text{VRD-KL}}$, which is formulated as:

$$\mathcal{L}_{\text{VRD-TS}} = \frac{1}{|\mathcal{B}|} \sum_{k=1}^{|\mathcal{B}|} \sum_{j=1}^{|\mathcal{B}|} I_k^{TS}[j] \log \frac{I_k^{TS}[j]}{T_k^{TS}[j]} \quad (22)$$

$$\mathcal{L}_{\text{VRD-ST}} = \frac{1}{|\mathcal{B}|} \sum_{k=1}^{|\mathcal{B}|} \sum_{j=1}^{|\mathcal{B}|} I_k^{ST}[j] \log \frac{I_k^{ST}[j]}{T_k^{ST}[j]} \quad (23)$$

$$\mathcal{L}_{\text{VRD-KL}} = \frac{1}{2} (\mathcal{L}_{\text{VRD-TS}} + \mathcal{L}_{\text{VRD-ST}}) \quad (24)$$

The total VRD loss is defined as the sum of $\mathcal{L}_{\text{VRD-CE}}$ and $\mathcal{L}_{\text{VRD-KL}}$. By jointly optimizing these two losses, VRD effectively transfers the teacher model’s representations and vertically-directed dependencies into the student.

$$\mathcal{L}_{\text{VRD}} = \mathcal{L}_{\text{VRD-CE}} + \mathcal{L}_{\text{VRD-KL}} \quad (25)$$

3.4 Cross Relational Distillation (XRD)

We further introduce a new distillation method, Cross Relational Distillation (XRD), to effectively transfer cross-modal relational knowledge. XRD aligns inter-modality similarity distributions (image-text and text-image), as illustrated in Figure 1-(c). Most conventional distillation methods focus on feature-level or intra-modality alignment. However, our method captures the bidirectional relationships between image and text representations of teacher and student. Specifically, XRD consists of four pairwise similarity distributions: $\mathcal{R}^{T_i \rightarrow S_i}$ teacher-image to student-text pairwise similarity distribution, $\mathcal{R}^{T_i \rightarrow S_i}$ teacher-text to student-image pairwise similarity distribution, $\mathcal{R}^{S_i \rightarrow T_i}$ student-image to teacher-text pairwise similarity distribution, and $\mathcal{R}^{S_i \rightarrow T_i}$ student-text to teacher-image pairwise similarity distribution. Given the image and text embeddings and learnable temperature parameters, each similarity distribution is formulated as:

$$\mathcal{R}_k^{T_i \rightarrow S_i}[j] = \frac{\exp\left(v_k^T \cdot s_j^S / \tau\right)}{\sum_{b=1}^{|\mathcal{B}|} \exp\left(v_k^T \cdot s_b^S / \tau\right)} \quad (26)$$

$$\mathcal{R}_k^{T_i \rightarrow S_i}[j] = \frac{\exp\left(s_k^T \cdot v_j^S / \tau\right)}{\sum_{b=1}^{|\mathcal{B}|} \exp\left(s_k^T \cdot v_b^S / \tau\right)} \quad (27)$$

$$\mathcal{R}_k^{S_i \rightarrow T_i}[j] = \frac{\exp\left(v_k^S \cdot s_j^T / \tau\right)}{\sum_{b=1}^{|\mathcal{B}|} \exp\left(v_k^S \cdot s_b^T / \tau\right)} \quad (28)$$

$$\mathcal{R}_k^{S_i \rightarrow T_i}[j] = \frac{\exp\left(s_k^S \cdot v_j^T / \tau\right)}{\sum_{b=1}^{|\mathcal{B}|} \exp\left(s_k^S \cdot v_b^T / \tau\right)} \quad (29)$$

Each distribution represents the pairwise similarity between samples across the two modalities and two networks. The XRD loss consists of $\mathcal{L}_{T \rightarrow S}$ and $\mathcal{L}_{S \rightarrow T}$. $\mathcal{L}_{T \rightarrow S}$ minimizes the KL-divergence between teacher-to-student directed distributions, and $\mathcal{L}_{S \rightarrow T}$ minimizes that of student-to-teacher directed distributions. Unlike VRD, which aligns vertically-directed distributions, XRD aligns cross-modal dependencies, and therefore applies KL-divergence in both directions and averages the results to ensure symmetric alignment. Specifically, $\mathcal{L}_{T \rightarrow S}$ is obtained by computing KL-divergence between $\mathcal{R}_k^{T_i \rightarrow S_i}[j]$ and $\mathcal{R}_k^{T_i \rightarrow S_i}[j]$, and $\mathcal{L}_{S \rightarrow T}$ follows the same formulation applied to student-to-teacher directed distributions. Through this strategy, the student learns how each modality of one network semantically interacts with the other modality of the other network, thereby enabling richer cross-modal alignment. The formulas for $\mathcal{L}_{T \rightarrow S}$ and $\mathcal{L}_{S \rightarrow T}$ are as follows:

$$\mathcal{L}_{T \rightarrow S} = \frac{1}{2} \left(\frac{1}{|\mathcal{B}|} \sum_{k=1}^{|\mathcal{B}|} \sum_{j=1}^{|\mathcal{B}|} \mathcal{R}_k^{T_i \rightarrow S_i} [j] \log \frac{\mathcal{R}_k^{T_i \rightarrow S_i} [j]}{\mathcal{R}_k^{T_i \rightarrow S_i} [j]} \right. \\ \left. + \frac{1}{|\mathcal{B}|} \sum_{k=1}^{|\mathcal{B}|} \sum_{j=1}^{|\mathcal{B}|} \mathcal{R}_k^{T_i \rightarrow S_i} [j] \log \frac{\mathcal{R}_k^{T_i \rightarrow S_i} [j]}{\mathcal{R}_k^{T_i \rightarrow S_i} [j]} \right) \quad (30)$$

$$\mathcal{L}_{S \rightarrow T} = \frac{1}{2} \left(\frac{1}{|\mathcal{B}|} \sum_{k=1}^{|\mathcal{B}|} \sum_{j=1}^{|\mathcal{B}|} \mathcal{R}_k^{S_i \rightarrow T_i} [j] \log \frac{\mathcal{R}_k^{S_i \rightarrow T_i} [j]}{\mathcal{R}_k^{S_i \rightarrow T_i} [j]} \right. \\ \left. + \frac{1}{|\mathcal{B}|} \sum_{k=1}^{|\mathcal{B}|} \sum_{j=1}^{|\mathcal{B}|} \mathcal{R}_k^{S_i \rightarrow T_i} [j] \log \frac{\mathcal{R}_k^{S_i \rightarrow T_i} [j]}{\mathcal{R}_k^{S_i \rightarrow T_i} [j]} \right) \quad (31)$$

The overall XRD loss, \mathcal{L}_{XRD} , is obtained by averaging $\mathcal{L}_{T \rightarrow S}$ and $\mathcal{L}_{S \rightarrow T}$, and is formulated as:

$$\mathcal{L}_{\text{XRD}} = \frac{1}{2} (\mathcal{L}_{T \rightarrow S} + \mathcal{L}_{S \rightarrow T}) \quad (32)$$

This symmetric formulation further ensures bidirectional consistency between teacher and student relational mapping across modalities. Thus, the student model can learn the cross-modal structural knowledge captured by the teacher to improve semantic alignment between image and text embeddings. Consequently, as illustrated in Figure 1, HRD, VRD, and XRD together constitute a multi-directional relational distillation framework, enabling symmetric and balanced knowledge transfer from teacher to student.

3.5 CLIP-RD

Our framework, CLIP-RD, is trained by minimizing a joint loss function:

$$\mathcal{L}_{\text{CLIP-RD}} = \mathcal{L}_{\text{task}} + \alpha \mathcal{L}_{\text{FD}} + \beta \mathcal{L}_{\text{ICL}} + \lambda \mathcal{L}_{\text{RD}} \quad (33)$$

where $\mathcal{L}_{\text{RD}} \in \{\mathcal{L}_{\text{HRD}}, \mathcal{L}_{\text{VRD}}, \mathcal{L}_{\text{XRD}}\}$. α , β , and λ are hyperparameters that balance the contributions of the different loss terms. In all experiments, we set $\alpha = 2000$, $\beta = 1$, and $\lambda = 1$ for all relational distillation losses, adopting the optimal scaling factors for \mathcal{L}_{FD} , \mathcal{L}_{ICL} , and \mathcal{L}_{HRD} reported in [52]. This framework, $\mathcal{L}_{\text{CLIP-RD}}$, delivers relational knowledge for more robust student models.

4 Experiments

4.1 Experimental Setup

4.1.1 Architecture

The original CLIP [34] framework employs a Transformer[43] as the text encoder and utilizes Vision

Transformer (ViT) [10] as the image encoder. Following this paradigm, our proposed CLIP-RD adopts an identical architectural configuration. For the knowledge distillation process, we employ ViT-B/16 as the teacher model; specifically, we utilize the pre-trained checkpoints provided by CLIP-KD [52] as our starting point for the teacher. For distillation, we use ViT-T/16 as the student model. The detailed configurations of visual and text encoders are presented in Supplementary Materials, following the OpenCLIP [37] codebase.

4.1.2 Dataset

The teacher model is initialized from CLIP-KD [52] checkpoints pre-trained on LAION-400M [38]. For distilling the vision-language student model, we use Conceptual Captions 3M (CC3M) [39] and 12M (CC12M) [3] following the official annotation files. Images are downloaded from the provided URLs, and samples with inaccessible images are filtered out. After filtering, CC3M contains 2,230,103 training samples and 10,669 validation samples, while CC12M consists of 7,215,613 training samples.

For zero-shot classification evaluation, we use the ImageNet [9] validation set along with its distribution-shifted variants: ImageNet-V2 (IN-V2) [35], ImageNet-Rendition (IN-R) [18], and ImageNet-Sketch (IN-S) [45], reporting the top-1 accuracy. For zero-shot cross-modal retrieval, we evaluate on MSCOCO [29] and Flickr30K [53] following the standard Karpathy split [23], reporting Recall@1 (R@1) for both Image-to-Text (I2T) and Text-to-Image (T2I). In addition, we evaluate zero-shot performance on a diverse set of benchmark datasets, including CIFAR-10/100 [26], EuroSAT [17], RESISC45 [5], Food101 [2], Sun397 [51], and Caltech101 [14].

4.1.3 Training details

We train the models for 32 epochs with a 10K iteration warmup, followed by a cosine learning rate decay schedule. Optimization is performed using AdamW [30], following the configuration of CLIP-KD, with an initial learning rate of 0.001 and a weight decay of 0.1. The global batch size is set to 1,024 across 8 workers. All learnable temperature parameters are initialized to 0.07 following CLIP-KD and the original CLIP.

Experiments are conducted on NVIDIA RTX PRO 6000 Blackwell GPUs. For other implementation details not explicitly specified, we follow the standard training protocols of CLIP-KD.

4.2 Distilling CLIP Models

We demonstrate the robustness of CLIP-RD through distillation experiments on two different student networks, evaluating on both zero-shot classification and retrieval tasks.

Table 1: Comparison with existing CLIP distillation methods. A star (*) denotes results reproduced using the official implementation.

Method	IN-1K	MSCOCO		Flickr	
		I2T	T2I	I2T	T2I
T: ViT-B/16	67.1	39.5	36.5	76.5	75.5
S: ViT-T/16	29.3	18.2	17.9	39.3	42.0
TinyCLIP	40.8	26.8	24.7	58.6	58.5
CLIP-KD*	41.3	27.4	24.1	58.4	56.4
CLIP-RD (Ours)	42.1	27.8	25.1	58.3	58.6

Table 2: Zero-shot classification and retrieval performance comparison.

Method	IN-1K	IN-V2	IN-R	IN-S	CC3M	
					I2T	T2I
T: ViT-B/16	67.1	59.6	77.9	52.4	42.8	42.2
S: ViT-T/16	29.3	24.9	34.2	16.9	33.6	34.0
CLIP-KD	41.3	35.5	46.3	26.3	40.2	38.7
CLIP-RD (Ours)	42.1	36.2	48.3	27.3	40.6	39.3

4.2.1 Zero-Shot Classification

In Table 1, we evaluate CLIP-RD on ImageNet zero-shot classification. We conduct experiments with a student architecture: ViT-T/16, compared against TinyCLIP, and CLIP-KD. The performance of TinyCLIP is reported from the results presented in CLIP-KD [52]. It should also be noted that the training data used to train TinyCLIP is about 2.7M more image-text pairs than the training data used to train CLIP-KD and CLIP-RD in our experiments. We reproduce CLIP-KD using its official implementation and mark the result with a star (*). CLIP-RD achieves 42.1% accuracy and outperforms the baseline of ViT-T/16 by 12.8%*p*. Furthermore, CLIP-RD outperforms TinyCLIP by 1.3%*p* and CLIP-KD by 0.8%*p*. These results demonstrate that our multi-directional relational distillation framework effectively maximizes the alignment of the student’s representation space, leading to enhanced ImageNet zero-shot classification performance. We additionally evaluate on ImageNet variant datasets, where CLIP-RD consistently outperforms CLIP-KD across all datasets by 0.7%*p* ~ 2.0%*p*, as shown in Table 2. These results demonstrate that our method effectively transfers CLIP’s strong generalization capability from teacher to student.

4.2.2 Cross-modal retrieval

Table 1 shows that we efficiently transfer knowledge from the teacher model to the student model for zero-shot cross-modal retrieval on MSCOCO and Flickr. Using ViT-B/16 as a teacher model, we observe improved zero-shot

Table 3: Zero-shot classification accuracy on various datasets.

Method	IN	CIFAR-10	CIFAR-100	EuroSAT	Food101	RESISC45	Sun397	Caltech101
T: ViT-B/16	67.1	91.1	71.3	33.8	80.2	57.8	69.0	87.0
S: ViT-T/16	29.3	66.9	27.5	11.6	27.8	24.4	38.1	66.2
CLIP-KD	41.3	74.2	39.9	18.0	41.6	32.6	51.6	75.9
CLIP-RD (Ours)	42.1	75.5	42.3	25.5	43.2	32.6	52.0	78.0

cross-modal retrieval performance of the student model. On MSCOCO, CLIP-RD improves I2T retrieval R@1 by 9.6%*p* over the ViT-T/16 baseline and by 1.0%*p* over TinyCLIP [49]. Moreover, it achieves a further improvement of 0.4%*p* compared to CLIP-KD. For T2I retrieval, our framework also outperforms CLIP-KD by 1.0%*p*. We observe similar trends on Flickr, where CLIP-RD yields improved retrieval performance. Specifically, CLIP-RD improves T2I retrieval by 2.2%*p*, compared to CLIP-KD. These results demonstrate that our framework provides an improvement in zero-shot cross-modal retrieval performance. We also report cross-modal retrieval performance on CC3M in Table 2. CLIP-RD outperforms CLIP-KD on I2T retrieval R@1 by 0.4%*p* and on T2I retrieval R@1 by 0.6%*p*.

4.2.3 Zero-shot classification on Various Datasets

We evaluate zero-shot image classification performance across diverse datasets to assess the robustness of our model. Specifically, we select 8 datasets that were originally used to evaluate zero-shot performance in CLIP. We compare the student baseline, CLIP-KD, and our proposed CLIP-RD.

As shown in Table 3, our proposed CLIP-RD outperforms CLIP-KD by up to 7.5%*p* across all datasets. On object classification benchmarks such as CIFAR-10/100 and Caltech101, it surpasses CLIP-KD by 1.3%*p* ~ 2.4%*p*. Notably, on EuroSAT, a challenging satellite image dataset, CLIP-RD demonstrates a substantial improvement of 7.5%*p*. On the fine-grained classification dataset, Food101, our model achieves improvements of 1.6%*p*. Also, our method achieves 0.4%*p* gain over CLIP-KD on the scene understanding benchmark, Sun397. These results indicate that our model delivers strong and robust zero-shot performance across diverse datasets.

4.3 Ablation Study

Table 4 examines the effectiveness of Vertical Relational Distillation (VRD), Cross Relational Distillation (XRD), and the CLIP-RD approach with zero-shot ImageNet-1K classification and cross-modal retrieval (MSCOCO, Flickr) performance.

First, CLIP-KD+XRD shows an accuracy of 41.9% on IN-1K, which is a 0.6%*p* improvement over CLIP-KD, and on MSCOCO and Flickr, it demonstrates performance

Table 4: Ablation study.

Method	IN-1K	MSCOCO		Flickr	
		I2T	T2I	I2T	T2I
T: ViT-B/16	67.1	39.5	36.5	76.5	75.5
S: ViT-T/16	29.3	18.2	17.9	39.3	42.0
CLIP-KD	41.3	27.4	24.1	58.4	56.4
CLIP-KD+XRD	41.9	27.6	24.8	59.5	57.7
CLIP-KD+VRD	42.0	27.6	25.0	61.0	58.6
CLIP-RD	42.1	27.8	25.1	58.3	58.6

gains of 0.2%/0.7%*p* (I2T/T2I) and 1.1%/1.3%*p*, respectively. CLIP-KD+VRD also achieves 42.0% accuracy on IN-1K, which is a 0.7%*p* improvement over CLIP-KD (41.3%), and on MSCOCO and Flickr, it shows performance enhancement of 0.2%/0.9%*p* and 2.6%/2.2%*p* respectively, exhibiting consistent performance improvements overall.

We further combine CLIP-KD, VRD, and XRD to investigate our final relation-based distillation framework, CLIP-RD. CLIP-RD achieves 42.1% accuracy on IN-1K, 27.8%/25.1% and 58.3%/58.6% on MSCOCO and Flickr, respectively. This demonstrates additional performance improvements compared to applying them individually, which suggests that vertical and cross relational information complement each other, allowing for richer relational knowledge to be conveyed to the student model.

Overall, we can confirm that the two relation-based distillation strategies complement each other and CLIP-KD. Furthermore, CLIP-RD efficiently enhances the representational expressiveness of the student model.

5 Conclusion

In this paper, we propose CLIP-RD, introducing two novel relational distillation strategies: VRD and XRD. VRD enforces consistency of teacher–student distillation strength across modalities at the distribution level, while XRD imposes bidirectional symmetry on cross-modal teacher–student similarity distributions. These two strategies are complementary to each other and to prior distillation objectives, jointly strengthening relational consistency between teacher and student representations. Extensive experiments and ablation studies demonstrate that emphasizing relational structures within the image–text embedding space between teacher and student models significantly enhances the performance of multimodal knowledge distillation. We hope that this work inspires future research on knowledge distillation methods that more effectively leverage the intrinsic relational characteristics of CLIP-like models.

References

- [1] Bansal, A., Sikka, K., Sharma, G., Chellappa, R., Divakaran, A.: Zero-shot object detection. In: Proceedings of the European conference on computer vision (ECCV). pp. 384–400 (2018)
- [2] Bossard, L., Guillaumin, M., Van Gool, L.: Food-101 – mining discriminative components with random forests. In: European Conference on Computer Vision (2014)
- [3] Changpinyo, S., Sharma, P., Ding, N., Soricut, R.: Conceptual 12m: Pushing web-scale image-text pre-training to recognize long-tail visual concepts. In: Proceedings of the IEEE/CVF conference on computer vision and pattern recognition. pp. 3558–3568 (2021)
- [4] Chen, K., Wu, X.: Vtqa: Visual text question answering via entity alignment and cross-media reasoning. In: Proceedings of the IEEE/CVF Conference on Computer Vision and Pattern Recognition. pp. 27218–27227 (2024)
- [5] Cheng, G., Han, J., Lu, X.: Remote sensing image scene classification: Benchmark and state of the art. Proceedings of the IEEE **105**(10), 1865–1883 (2017)
- [6] Csizmadia, D., Codreanu, A., Sim, V., Prabhu, V., Lu, M., Zhu, K., O’Brien, S., Sharma, V.: Distill clip (dclip): Enhancing image-text retrieval via cross-modal transformer distillation. arXiv preprint arXiv:2505.21549 (2025)
- [7] Dai, W., Hou, L., Shang, L., Jiang, X., Liu, Q., Fung, P.: Enabling multimodal generation on clip via vision-language knowledge distillation. In: Findings of the Association for Computational Linguistics: ACL 2022. pp. 2383–2395 (2022)
- [8] Dancette, C., Whitehead, S., Maheshwary, R., Vedantam, R., Scherer, S., Chen, X., Cord, M., Rohrbach, M.: Improving selective visual question answering by learning from your peers. In: Proceedings of the IEEE/CVF Conference on Computer Vision and Pattern Recognition. pp. 24049–24059 (2023)
- [9] Deng, J., Dong, W., Socher, R., Li, L.J., Li, K., Fei-Fei, L.: Imagenet: A large-scale hierarchical image database. In: 2009 IEEE conference on computer vision and pattern recognition. pp. 248–255. Ieee (2009)
- [10] Dosovitskiy, A., Beyer, L., Kolesnikov, A., Weissenborn, D., Zhai, X., Unterthiner, T., Dehghani, M.,

- Minderer, M., Heigold, G., Gelly, S., et al.: An image is worth 16x16 words: Transformers for image recognition at scale. *arXiv preprint arXiv:2010.11929* (2020)
- [11] Eom, S., Ho, N., Oh, J., Yun, S.Y.: Cross-modal retrieval meets inference: Improving zero-shot classification with cross-modal retrieval. *arXiv preprint arXiv:2308.15273* (2023)
- [12] Eslami, S., de Melo, G.: Mitigate the gap: Investigating approaches for improving cross-modal alignment in clip. *arXiv preprint arXiv:2406.17639* (2024)
- [13] Fang, Z., Wang, J., Hu, X., Wang, L., Yang, Y., Liu, Z.: Compressing visual-linguistic model via knowledge distillation. In: *Proceedings of the IEEE/CVF International Conference on Computer Vision*. pp. 1428–1438 (2021)
- [14] Fei-Fei, L., Fergus, R., Perona, P.: Learning generative visual models from few training examples: An incremental bayesian approach tested on 101 object categories. *Computer vision and Image understanding* **106**(1), 59–70 (2007)
- [15] Ge, Y., Ren, J., Gallagher, A., Wang, Y., Yang, M.H., Adam, H., Itti, L., Lakshminarayanan, B., Zhao, J.: Improving zero-shot generalization and robustness of multi-modal models. In: *Proceedings of the IEEE/CVF conference on computer vision and pattern recognition*. pp. 11093–11101 (2023)
- [16] He, K., Zhang, X., Ren, S., Sun, J.: Deep residual learning for image recognition. In: *Proceedings of the IEEE conference on computer vision and pattern recognition*. pp. 770–778 (2016)
- [17] Helber, P., Bischke, B., Dengel, A., Borth, D.: Eurosat: A novel dataset and deep learning benchmark for land use and land cover classification. *IEEE Journal of Selected Topics in Applied Earth Observations and Remote Sensing* **12**(7), 2217–2226 (2019)
- [18] Hendrycks, D., Basart, S., Mu, N., Kadavath, S., Wang, F., Dorundo, E., Desai, R., Zhu, T., Parajuli, S., Guo, M., et al.: The many faces of robustness: A critical analysis of out-of-distribution generalization. In: *Proceedings of the IEEE/CVF international conference on computer vision*. pp. 8340–8349 (2021)
- [19] Hinton, G., Vinyals, O., Dean, J.: Distilling the knowledge in a neural network. *arXiv preprint arXiv:1503.02531* (2015)
- [20] Huang, C., Seto, S., Abnar, S., Grangier, D., Jaitly, N., Susskind, J.: Aggregate-and-adapt natural language prompts for downstream generalization of clip. *Advances in Neural Information Processing Systems* **37**, 81077–81104 (2024)
- [21] Jiao, X., Yin, Y., Shang, L., Jiang, X., Chen, X., Li, L., Wang, F., Liu, Q.: Tinybert: Distilling bert for natural language understanding. In: *Findings of the association for computational linguistics: EMNLP 2020*. pp. 4163–4174 (2020)
- [22] Kaplan, J., McCandlish, S., Henighan, T., Brown, T.B., Chess, B., Child, R., Gray, S., Radford, A., Wu, J., Amodei, D.: Scaling laws for neural language models. *arXiv preprint arXiv:2001.08361* (2020)
- [23] Karpathy, A., Fei-Fei, L.: Deep visual-semantic alignments for generating image descriptions. In: *Proceedings of the IEEE conference on computer vision and pattern recognition*. pp. 3128–3137 (2015)
- [24] Kim, J., Chang, S., Kwak, N.: Pqk: model compression via pruning, quantization, and knowledge distillation. *arXiv preprint arXiv:2106.14681* (2021)
- [25] Kim, T., Oh, J., Kim, N., Cho, S., Yun, S.Y.: Comparing kullback-leibler divergence and mean squared error loss in knowledge distillation. *arXiv preprint arXiv:2105.08919* (2021)
- [26] Krizhevsky, A., Hinton, G., et al.: Learning multiple layers of features from tiny images. *Tech. rep., Department of Computer Science, University of Toronto* (2009)
- [27] Kuo, W., Cui, Y., Gu, X., Piergiovanni, A., Angelova, A.: F-vlm: Open-vocabulary object detection upon frozen vision and language models. *arXiv preprint arXiv:2209.15639* (2022)
- [28] Li, Z., Li, X., Fu, X., Zhang, X., Wang, W., Chen, S., Yang, J.: Promptkd: Unsupervised prompt distillation for vision-language models. In: *Proceedings of the IEEE/CVF Conference on Computer Vision and Pattern Recognition*. pp. 26617–26626 (2024)
- [29] Lin, T.Y., Maire, M., Belongie, S., Hays, J., Perona, P., Ramanan, D., Dollár, P., Zitnick, C.L.: Microsoft coco: Common objects in context. In: *European conference on computer vision*. pp. 740–755. Springer (2014)
- [30] Loshchilov, I., Hutter, F.: Decoupled weight decay regularization. *arXiv preprint arXiv:1711.05101* (2017)
- [31] Mirzadeh, S.I., Farajtabar, M., Li, A., Levine, N., Matsukawa, A., Ghasemzadeh, H.: Improved knowledge distillation via teacher assistant. In: *Proceedings of the AAAI conference on artificial intelligence*. vol. 34, pp. 5191–5198 (2020)

- [32] Peng, Z., Dong, L., Bao, H., Ye, Q., Wei, F.: Beit v2: Masked image modeling with vector-quantized visual tokenizers. *arXiv preprint arXiv:2208.06366* (2022)
- [33] Pham, H., Dai, Z., Ghiasi, G., Kawaguchi, K., Liu, H., Yu, A.W., Yu, J., Chen, Y.T., Luong, M.T., Wu, Y., et al.: Combined scaling for zero-shot transfer learning. *Neurocomputing* **555**, 126658 (2023)
- [34] Radford, A., Kim, J.W., Hallacy, C., Ramesh, A., Goh, G., Agarwal, S., Sastry, G., Askell, A., Mishkin, P., Clark, J., et al.: Learning transferable visual models from natural language supervision. In: *International conference on machine learning*. pp. 8748–8763. PmLR (2021)
- [35] Recht, B., Roelofs, R., Schmidt, L., Shankar, V.: Do imagenet classifiers generalize to imagenet? In: *International conference on machine learning*. pp. 5389–5400. PMLR (2019)
- [36] Sanh, V., Debut, L., Chaumond, J., Wolf, T.: Distilbert, a distilled version of bert: smaller, faster, cheaper and lighter. *arXiv preprint arXiv:1910.01108* (2019)
- [37] Schuhmann, C., Beaumont, R., Vencu, R., Gordon, C.W., Wightman, R., Cherti, M., Coombes, T., Katta, A., Mullis, C., Wortsman, M., Schramowski, P., Kundurthy, S.R., Crowson, K., Schmidt, L., Kaczmarczyk, R., Jitsev, J.: LAION-5b: An open large-scale dataset for training next generation image-text models. In: *Thirty-sixth Conference on Neural Information Processing Systems Datasets and Benchmarks Track* (2022)
- [38] Schuhmann, C., Vencu, R., Beaumont, R., Kaczmarczyk, R., Mullis, C., Katta, A., Coombes, T., Jitsev, J., Komatsuzaki, A.: Laion-400m: Open dataset of clip-filtered 400 million image-text pairs. *arXiv preprint arXiv:2111.02114* (2021)
- [39] Sharma, P., Ding, N., Goodman, S., Soricut, R.: Conceptual captions: A cleaned, hypernymed, image alt-text dataset for automatic image captioning. In: *Proceedings of the 56th Annual Meeting of the Association for Computational Linguistics (Volume 1: Long Papers)*. pp. 2556–2565 (2018)
- [40] Tan, C., Xu, X., Shen, F.: A survey of zero shot detection: Methods and applications. *Cognitive Robotics* **1**, 159–167 (2021)
- [41] Tan, M., Le, Q.: Efficientnet: Rethinking model scaling for convolutional neural networks. In: *International conference on machine learning*. pp. 6105–6114. PMLR (2019)
- [42] Touvron, H., Cord, M., Douze, M., Massa, F., Sablayrolles, A., Jégou, H.: Training data-efficient image transformers & distillation through attention. In: *International conference on machine learning*. pp. 10347–10357. PMLR (2021)
- [43] Vaswani, A., Shazeer, N., Parmar, N., Uszkoreit, J., Jones, L., Gomez, A.N., Kaiser, L., Polosukhin, I.: Attention is all you need. *Advances in neural information processing systems* **30** (2017)
- [44] Wan, Z., Wang, X., Liu, C., Alam, S., Zheng, Y., Liu, J., Qu, Z., Yan, S., Zhu, Y., Zhang, Q., et al.: Efficient large language models: A survey. *arXiv preprint arXiv:2312.03863* (2023)
- [45] Wang, H., Ge, S., Lipton, Z., Xing, E.P.: Learning robust global representations by penalizing local predictive power. *Advances in neural information processing systems* **32** (2019)
- [46] Wang, Z., Codella, N., Chen, Y.C., Zhou, L., Yang, J., Dai, X., Xiao, B., You, H., Chang, S.F., Yuan, L.: Clip-td: Clip targeted distillation for vision-language tasks. *arXiv preprint arXiv:2201.05729* (2022)
- [47] Wang, Z., Liang, J., He, R., Xu, N., Wang, Z., Tan, T.: Improving zero-shot generalization for clip with synthesized prompts. *arXiv preprint arXiv:2307.07397* (2023)
- [48] Wei, L., Xie, L., Zhou, W., Li, H., Tian, Q.: Mvp: Multimodality-guided visual pre-training. In: *European conference on computer vision*. pp. 337–353. Springer (2022)
- [49] Wu, K., Peng, H., Zhou, Z., Xiao, B., Liu, M., Yuan, L., Xuan, H., Valenzuela, M., Chen, X.S., Wang, X., et al.: Tinyclip: Clip distillation via affinity mimicking and weight inheritance. In: *Proceedings of the IEEE/CVF International Conference on Computer Vision*. pp. 21970–21980 (2023)
- [50] Wu, K., Zhang, J., Peng, H., Liu, M., Xiao, B., Fu, J., Yuan, L.: Tinyvit: Fast pretraining distillation for small vision transformers. In: *European conference on computer vision*. pp. 68–85. Springer (2022)
- [51] Xiao, J., Hays, J., Ehinger, K.A., Oliva, A., Torralba, A.: Sun database: Large-scale scene recognition from abbey to zoo. In: *2010 IEEE computer society conference on computer vision and pattern recognition*. pp. 3485–3492. IEEE (2010)
- [52] Yang, C., An, Z., Huang, L., Bi, J., Yu, X., Yang, H., Diao, B., Xu, Y.: Clip-kd: An empirical study of clip model distillation. In: *Proceedings of the IEEE/CVF Conference on Computer Vision and Pattern Recognition*. pp. 15952–15962 (2024)

- [53] Young, P., Lai, A., Hodosh, M., Hockenmaier, J.: From image descriptions to visual denotations: New similarity metrics for semantic inference over event descriptions. *Transactions of the association for computational linguistics* **2**, 67–78 (2014)
- [54] Zhai, X., Wang, X., Mustafa, B., Steiner, A., Keysers, D., Kolesnikov, A., Beyer, L.: Lit: Zero-shot transfer with locked-image text tuning. In: *Proceedings of the IEEE/CVF conference on computer vision and pattern recognition*. pp. 18123–18133 (2022)
- [55] Zhang, S.H., Tang, W.C., Wu, C., Hu, P., Li, N., Zhang, L.J., Zhang, Q., Zhang, S.Q.: Ternaryclip: Efficiently compressing vision-language models with ternary weights and distilled knowledge. *arXiv preprint arXiv:2510.21879* (2025)
- [56] Zhou, K., Yang, J., Loy, C.C., Liu, Z.: Learning to prompt for vision-language models. *International journal of computer vision* **130**(9), 2337–2348 (2022)

A Implementation Details

Table 5 presents the configurations of the image and text encoders used in our experiments. It includes the networks used in both the main experiments and the additional experiments described below. We use ViT-B/16 as the teacher model, while the other models serve as students.

Table 5: Configuration of paired visual and text encoder.

Model	Visual encoder		Text encoder: Transformer[43]			
	Type	Params	Layer	Width	Head	Params
ViT-B/16 [10]	ViT	86.2M	12	512	8	37.8M
ViT-T/16 [10]		5.6M	12	384	6	21.3M
ResNet-50 [16]	CNN	38.3M	12	512	8	37.8M
ResNet-18 [16]		11.4M	12	384	6	21.3M
EfficientNet-B0 [41]		4.7M	12	384	6	21.3M

B Additional Experiments

In additional experiments, we employ three CNN models with large, medium, and small parameter sizes to vary the visual encoder capacity and evaluate zero-shot classification on ImageNet and its variants and retrieval performance on CC3M [39], MSCOCO [29], and Flickr [53].

B.1 Zero-shot Classification with CNN

Table 6: Zero-shot classification with CNN.

Method	IN-1K	IN-V2	IN-R	IN-S
T: ViT-B/16	67.1	59.6	77.9	52.4
S: ResNet-50	34.8	29.6	45.9	24.4
CLIP-KD	54.1	46.6	66.0	41.6
CLIP-RD (Ours)	55.1	47.2	66.9	42.3
S: ResNet-18	27.3	22.8	35.0	18.0
CLIP-KD	38.2	31.9	45.0	25.8
CLIP-RD (Ours)	38.6	31.9	46.2	26.2
S: EfficientNet-B0	30.9	26.4	39.8	18.0
CLIP-RD (Ours)	46.1	38.8	55.4	33.3

We evaluate the zero-shot classification performance of CLIP-RD using CNN architectures on ImageNet and its variants: ImageNet-1K (IN) [9], ImageNet-V2 (IN-V2) [35], ImageNet-Rendition (IN-R) [18], and ImageNet-Sketch (IN-S) [45]. As shown in Table 6, CLIP-RD consistently improves performance over CLIP-KD across all datasets. Moreover, CLIP-RD significantly surpasses baseline student models by 8.3%p ~ 21.0%p, demonstrating larger gains than CLIP-KD. In particular, IN-R and IN-S exhibit substantially larger domain shifts from the original ImageNet distribution. CLIP-RD achieves notable improvements on these more challenging OOD

datasets, suggesting that relational distillation is particularly beneficial under significant distribution shifts.

B.2 Zero-shot Retrieval with CNN

We also assess zero-shot cross-modal retrieval performance on CC3M, MSCOCO, and Flickr. In Table 7, CLIP-RD outperforms CLIP-KD in most tasks by up to 0.7%p. CLIP-RD surpasses the baseline models, yielding gains from 3.6%p to 20.8%p across different architectures. We demonstrate that our method effectively transfers CLIP’s strong zero-shot retrieval capability from teacher to student.

Table 7: Zero-shot retrieval with CNN.

Method	CC3M		MSCOCO		Flickr	
	I2T	T2I	I2T	T2I	I2T	T2I
T: ViT-B/16	43.8	42.2	39.5	36.5	76.5	75.5
S: ResNet-50	40.7	39.6	23.2	22.9	52.2	52.7
CLIP-KD	47.1	45.3	36.0	32.9	74.9	69.4
CLIP-RD (Ours)	47.2	45.7	36.6	32.9	73.0	70.4
S: ResNet-18	31.7	30.9	16.2	16.4	43.6	41.5
CLIP-KD	36.9	34.1	25.5	21.6	56.6	52.4
CLIP-RD (Ours)	37.6	34.5	25.6	22.0	54.4	52.7
S: EfficientNet-B0	36.3	36.7	20.8	20.3	44.9	47.2
CLIP-RD (Ours)	42.8	41.0	30.9	27.3	64.3	62.7

C Analysis

We analyze our framework in several ways using ViT-B/16 pre-trained on LAION-400M [38] as the teacher model and ViT-T/16 distilled using CC3M [39] and CC12M [3] datasets as the student model. The following analyses provide a deeper understanding of the proposed method.

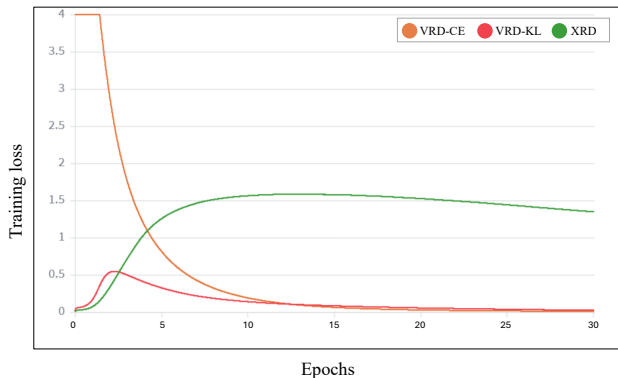


Figure 2: Training loss. The y-axis is clipped at 4.0 to emphasize relative trends after the initial warm-up phase.

C.1 Loss Analysis

We conduct a loss analysis by measuring the training losses over epochs, with results shown in Figure 2. As illustrated, \mathcal{L}_{VRD-CE} , \mathcal{L}_{VRD-KL} , and \mathcal{L}_{XRD} all decrease as training progresses. Notably, although \mathcal{L}_{VRD-KL} and \mathcal{L}_{XRD} initially increase from very small values, they quickly stabilize and subsequently decrease. This indicates that our proposed strategies train the model in a stable and consistent manner.

C.2 Training Curves Analysis

We analyze the training performance curves of ImageNet top-1/top-5 accuracy and CC3M I2T/T2I R@1. As illustrated in Figure 3, CLIP-RD consistently achieves higher performance than CLIP-KD on both ImageNet and CC3M across all metrics and anchors. These results demonstrate the stability and robustness of our method throughout the training process.

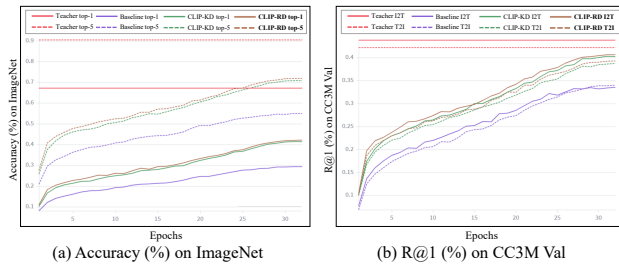


Figure 3: Accuracy on IN and R@1 on CC3M Val.

C.3 Similarity Distribution Analysis

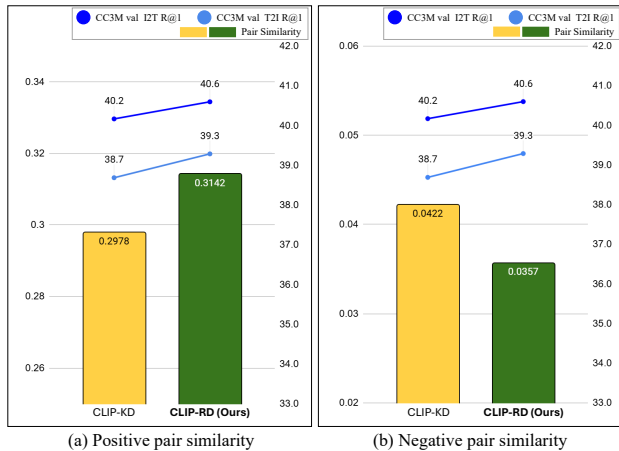


Figure 4: Positive and negative pair similarity and CC3M validation set retrieval performance with CLIP-KD and CLIP-RD.

We compare positive and negative pair similarities between CLIP-KD and our method on the CC3M validation

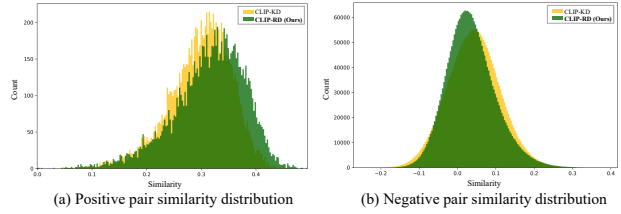


Figure 5: Positive and negative pair similarity distribution with CLIP-KD and CLIP-RD. As in Figure 4, higher positive (a) and lower negative (b) similarity indicate better alignment for representation space.

subset. Specifically, we compute the average cosine similarity across all positive pairs and all negative pairs, respectively. Higher positive pair similarity and lower negative pair similarity indicate a more discriminative representation space with clearer boundaries between positive and negative pairs.

As illustrated in Figure 4, CLIP-RD achieves higher positive pair similarity and lower negative pair similarity than CLIP-KD, indicating that our method pulls positive pairs closer while pushing negative pairs further apart. This is also consistent with the CC3M retrieval results.

We further compare the distributions of positive and negative pair similarities in Figure 5. The positive pair similarity distribution shifts toward higher values compared to CLIP-KD, while the negative pair similarity distribution shifts toward lower values, demonstrating that our method effectively maximizes the alignment of the student’s representation space.

Finally, we compare the positive-negative similarity gap between CLIP-KD and our method, defined as the difference between the mean positive and mean negative similarities over training epochs. This metric reflects the overall level of discriminability between positive and negative pairs. As shown in Figure 6, CLIP-RD consistently outperforms CLIP-KD across most epochs, indicating that our method maintains superior alignment throughout training.

C.4 Lower Bound of Mutual Information : Formulaic Insight of VRD-CE Loss

Let $v^S \sim \mu(v^S), v^T \sim \mu(v^T)$ denote the student and teacher image embeddings. The joint distribution of positive pairs is $\mu(v^S, v^T)$ while negative pairs are sampled from the product of marginals $\mu(v^S)\mu(v^T)$. We introduce a binary variable $C \in \{0, 1\}$ where $C = 1$: positive pair, $C = 0$: negative pair.

$$\begin{aligned} \eta(v^S, v^T | C = 1) &= \mu(v^S, v^T) \\ \eta(v^S, v^T | C = 0) &= \mu(v^S)\mu(v^T) \end{aligned} \quad (34)$$

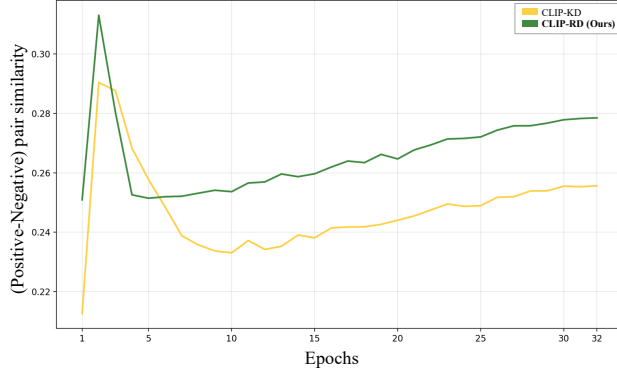


Figure 6: (Pos-neg) pair similarity.

For each positive pair, there are N negative pairs. The prior probabilities of C are:

$$\eta(C = 1) = \frac{1}{1 + N}, \quad \eta(C = 0) = \frac{N}{1 + N} \quad (35)$$

for $N = \mathcal{B} - 1$.

By Bayes' theorem,

$$\begin{aligned} \eta(C = 1|v^S, v^T) &= \frac{\eta(v^S, v^T|C = 1)}{\eta(v^S, v^T|C = 1)\eta(C = 1) + \eta(v^S, v^T|C = 0)\eta(C = 0)} \\ &= \frac{\mu(v^S, v^T)}{\mu(v^S, v^T) + N\mu(v^S)\mu(v^T)} \end{aligned} \quad (36)$$

The log-posterior can be written as:

$$\begin{aligned} \log \eta(C = 1|v^S, v^T) &= \log \frac{\mu(v^S, v^T)}{\mu(v^S, v^T) + N\mu(v^S)\mu(v^T)} \\ &= -\log \left(1 + N \frac{\mu(v^S)\mu(v^T)}{\mu(v^S, v^T)} \right) \\ &\leq -\log N + \log \frac{\mu(v^S, v^T)}{\mu(v^S)\mu(v^T)} \end{aligned} \quad (37)$$

The expected log class posterior is related to the mutual information as follows:

$$\begin{aligned} \mathbb{E}_{\eta(v^S, v^T|C=1)} \log \eta(C = 1|v^S, v^T) &\leq -\log N + \mathbb{E}_{\mu(v^S, v^T)} \log \frac{\mu(v^S, v^T)}{\mu(v^S)\mu(v^T)} \\ \Leftrightarrow I(v^S, v^T) &\geq \log N - \mathcal{L}_{\text{InfoNCE}}(S \rightarrow T) \end{aligned} \quad (38)$$

where $I(v^S, v^T)$ denotes mutual information between v^S and v^T . Similarly,

$$\begin{aligned} \mathbb{E}_{\eta(v^T, v^S|C=1)} \log \eta(C = 1|v^T, v^S) &\leq -\log N + I(v^T, v^S) \\ \Leftrightarrow I(v^T, v^S) &\geq \log N - \mathcal{L}_{\text{InfoNCE}}(T \rightarrow S) \end{aligned} \quad (39)$$

By combine Eq.5 and Eq.6:

$$\begin{aligned} 2I(v^S; v^T) &\geq 2 \log N - \mathcal{L}_{\text{InfoNCE-Image}}(T \rightarrow S) \\ &\quad - \mathcal{L}_{\text{InfoNCE-Image}}(S \rightarrow T) \end{aligned} \quad (40)$$

The two directional InfoNCE-Image objectives provide lower bounds on the same mutual information. By combining the two directions, the symmetry objective maximizes a lower bound on the mutual information between teacher and student image representations.

Similarly,

$$\begin{aligned} 2I(s^S; s^T) &\geq 2 \log N - \mathcal{L}_{\text{InfoNCE-Text}}(T \rightarrow S) \\ &\quad - \mathcal{L}_{\text{InfoNCE-Text}}(S \rightarrow T) \end{aligned} \quad (41)$$

Each of the two directional InfoNCE-Text objectives provides a lower bound on the same mutual information. By jointly optimizing both directions, the symmetric objective maximizes a lower bound on the text mutual information between teacher and student text representations.

According to the InfoNCE bounds, the expected loss provides a lower bound on mutual information between teacher and student representations. Therefore, minimizing $\mathcal{L}_{\text{VRD-CE}}$ (Eq.21 in the manuscript) approximately maximizes lower bound of mutual information.

D Limitation

We were unable to use datasets as large as CC3M and CC12M used in CLIP-KD, which makes a strictly fair comparison difficult. These datasets are released as collections of web-crawled image URLs rather than the images themselves, and some URLs are no longer accessible due to link expiration or removal. As a result, the number of available training samples is 2.7M smaller than the data size used in CLIP-KD. Nevertheless, we retrained CLIP-KD using the data available to us and observed that our proposed method achieved superior performance. We expect that our approach would demonstrate even stronger performance when trained on datasets commonly used in the field of CLIP knowledge distillation.